Element-specific insight into ferromagnetic stability in UCoGe revealed by soft x-ray magnetic circular dichroism

Yukiharu Takeda[*]

Materials Sciences Research Center, Japan Atomic Energy Agency, 1-1-1 Kouto, Sayo-cho, Sayo-gun, Hyogo 679-5148, Japan

Jiří Pospíšil

Advanced Science Research Center, Japan Atomic Energy Agency, Tokai, Ibaraki 319-1195, Japan
and Department of Condensed Matter Physics, Faculty of Mathematics and Physics, Charles University, Ke Karlovu
5, 121 16 Prague 2, Czech Republic

Hiroshi Yamagami

Materials Sciences Research Center, Japan Atomic Energy Agency, 1-1-1 Kouto, Sayo-cho, Sayo-gun, Hyogo 679-5148, Japan
and Department of Physics, Kyoto Sangyo University, Motoyama, Kamigamo, Kita-Ku, Kyoto 603-8555, Japan

Etsuji Yamamoto and Yoshinori Haga

Advanced Science Research Center, Japan Atomic Energy Agency, Tokai, Ibaraki 319-1195, Japan

We investigated the element-specific electronic states and magnetic properties of ferromagnetic superconductor UCoGe and Ru-substituted U($Co_{0.88}Ru_{0.12}$)Ge using soft x-ray magnetic circular dichroism (XMCD) experiments at the absorption edges of U $N_{4,5}$, Co $L_{2,3}$, and Ge $L_{2,3}$. YCoGe, a nonmagnetic compound without the $5f$ electrons, was also examined as a reference material. The shapes of the XMCD spectra of UCoGe at the U N_5 and Ge $L_{2,3}$ edges are indistinguishably similar to those of U($Co_{0.88}Ru_{0.12}$)Ge. On the other hand, the XMCD spectral shape at the Co L_2 edge is very peculiar and is changed by the presence of the U $5f$ electrons and the Ru substitution. From the sum rule analysis for the XMCD spectra, it was found that the magnetic moments of the U $5f$ and Co $3d$ electrons in UCoGe and U($Co_{0.88}Ru_{0.12}$)Ge are aligned in the same direction under the present experimental conditions: $T = 5.5$–50 K and $\mu_0 H = 0$–10 T. Furthermore, not only in UCoGe and U($Co_{0.88}Ru_{0.12}$)Ge but even in the case of YCoGe, the Co $3d$ electrons have a large orbital magnetic moment, suggesting that the Co $3d$ electrons in these compounds are in a low-symmetry electronic environment originally. Through the T and $\mu_0 H$ dependence of the XMCD intensity, it was revealed that the magnetic properties at the Co site are not simply induced by the magnetism at the U site and that the Co $3d$ electrons play an important role in the stability of ferromagnetism. The present findings clearly demonstrate that the contribution of not only the U $5f$ electrons but also the Co $3d$ electrons is very crucial to understanding the complex physical properties of the U($Co_{1-x}Ru_x$)Ge system.

DOI: 10.1103/PhysRevB.108.085129

I. INTRODUCTION

The coexistence of ferromagnetic (FM) and superconductivity (SC) discovered in UGe_2 [1,2] under pressure, URhGe [3] and UCoGe [4] at ambient is one of the most attractive issues in the field of solid-state physics because of the suitable platform for investigating spin-triplet SC states. From vast exploration, it has been found that these three compounds share a number of intriguing characteristics of physical properties, as summarized in Refs. [5] and [6]. UGe_2 crystallizes in the $ZrGa_2$-type orthorhombic structure. Meanwhile, URhGe and UCoGe crystallize in the TiNiSi-type orthorhombic structure. The two kinds of crystal structures are very similar from the viewpoint that the U atoms form zigzag chains along the a axis [6]. All three U-based FM SCs are itinerant ferromagnets

with extremely strong Ising-like anisotropy. Among them, UCoGe possesses the lowest Curie temperature (T_{Curie}) of $\sim$ 3 K with a tiny spontaneous magnetic moment of $\sim 0.07\mu_B$ per formula unit (f.u.), pointing along the orthorhombic c axis. Upon cooling, the superconductivity sets in at $T_{SC} \sim 0.6$ K, and the coexistence of FM and SC is realized microscopically. As the origin of the coexistence of FM and SC in UCoGe, the spin triplet mediated by the Ising-type FM spin fluctuation has been evidenced by a detailed series of NMR and nuclear quadrupole resonance (NQR) experiments [7–11]. Through extensive exploration for a new candidate for the spin-triplet SC, eventually, UTe_2 [12], a nonmagnetic heavy fermion SC, was discovered and made a great impact on the field of solid-state physics. Common and different characteristics among the three FM SCs and UTe_2 have been stimulating further research for understanding the underlying physics [13].

The role of the transition metal (TM) d electrons is certainly important for understanding the unique behavior of

[*]ytakeda@spring8.or.jp

FM SCs, because the magnetism of the ternary U compounds is strictly sensitive to the chemical substitution of TM elements. Indeed, the magnetism of UCoGe is strongly affected by small Fe or Ru substitution for Co [14,15]. Although URuGe is a paramagnetic (PM) compound, the Ru substitution for Co, i.e., U(Co$_{1-x}$Ru$_x$)Ge, leads to an initial sharp enhancement of the T_{Curie} and a spontaneous magnetic moment. In the polycrystalline sample at $x \sim 0.1$, the maximum values of T_{Curie} and the spontaneous magnetic moment reach 8.6 K and ~ 0.1 μ_B/(f.u.), respectively, whereas the SC state rapidly vanishes even for $x > 0.01$ [16,17]. In the case of Ru and Co substitution for Rh of URhGe, i.e., U(Rh$_{1-x}$Ru$_x$)Ge and U(Rh$_{1-x}$Co$_x$)Ge, T_{Curie} increases from $T_{Curie} = 9.5$ K in URhGe and has the maximum values 10.6 and 20 K for the Ru and Co doping, respectively [18]. In contrast, the Si substitution for Ge, i.e., URh(Ge$_{1-x}$Si$_x$), has little effect on T_{Curie} [18]. The drastic changes in the magnetic properties by chemical substitution imply that the electronic states of TM d electrons play an important role in the magnetism of the system as well as the U $5f$ electrons [19–22].

The studies of the chemical substitution mentioned above indicate that the knowledge of magnetic structure at each atom site, including the TM site, is essential and important to understand the complicated physical properties of FM SCs. Experimental reports about the magnetic structure in UCoGe have been previously made by the polarized neutron diffraction (PND) experiment [23], the combined study of magnetic Compton scattering (MCS) experiment and soft x-ray magnetic circular dichroism (XMCD) experiment at the U $4d \rightarrow 5f$ ($N_{4,5}$) and Co $2p \rightarrow 3d$ ($L_{2,3}$) absorption edges [24] (hereafter denoted as U-$N_{4,5}$ and Co-$L_{2,3}$, respectively), and the hard x-ray XMCD experiment at the U $3d \rightarrow 5f$ (U-$M_{4,5}$) edge [25]. However, contradictions and unresolved issues about the orientation and magnitude of magnetic moments remain in the previous experimental results and their interpretations [26]. To unravel the chaotic situation, we consider that it is worth promoting high-precision XMCD experiments in soft x-ray regions, taking advantage of the feature that the magnetic structures and electronic states of the U $5f$ and Co $3d$ electrons can be treated simultaneously because Co-$L_{2,3}$ and U-$N_{4,5}$ coexist in the soft x-ray region.

In this paper, in order to investigate the element-specific electronic states and magnetic properties, and the effect of the Ru substitution for Co atoms, we performed soft x-ray XMCD experiments on UCoGe and U(Co$_{0.88}$Ru$_{0.12}$)Ge at U-$N_{4,5}$, Co-$L_{2,3}$, and Ge-$L_{2,3}$ in the range of temperature (T) and magnetic field ($\mu_0 H$, hereafter denoted simply as H), $T = 5.5 \sim 50$ K, and $H = 0 \sim 10$ Tesla (T), respectively. Here it should be emphasized that the single-crystal U(Co$_{0.88}$Ru$_{0.12}$)Ge possesses the highest value of T_{Curie} and the largest magnitude of magnetic moment as described later [28]. In addition, the XMCD experiment on YCoGe was also performed at Co-$L_{2,3}$ in order to reveal the electronic states of the Co $3d$ electrons which are not hybridized with the U $5f$ electrons in the TiNiSi-type orthorhombic structure [29]. We observed clear XMCD signals at U-$N_{4,5}$, Co-$L_{2,3}$, and Ge-$L_{2,3}$ for UCoGe and U(Co$_{0.88}$Ru$_{0.12}$)Ge. From the XMCD spectra, we concluded that the magnetic moments of the U $5f$ and Co $3d$ electrons are aligned in the same direction and are parallel to the applied H direction under all the present

experimental conditions. Furthermore, the peculiar shape of the XMCD spectra at Co-L_2 was observed, and the shape was changed due to the presence of the U $5f$ electrons and the Ru substitution. Reflecting the special shape of the XMCD spectra at Co-L_2, it was revealed that the Co $3d$ electrons in UCoGe, U(Co$_{0.88}$Ru$_{0.12}$)Ge, and even YCoGe have a large value of orbital magnetic moment (M_L), implying that the Co $3d$ electrons in the TiNiSi-type orthorhombic structure are originally in a low-symmetry electronic environment. From T and H dependence of the XMCD intensity at the U and Co sites, we found that the electronic states of the Co $3d$ electrons play a key role in the drastic changes in magnetism and the stability of the FM state in this system.

II. EXPERIMENTAL

The single-crystals of UCoGe, U(Co$_{0.88}$Ru$_{0.12}$)Ge [hereafter simply U(CoRu)Ge], and YCoGe used in the present study were grown by the Czochralski method. The crystal growth process is written in detail therein [16,17,28]. The value of T_{Curie} of the single-crystal U(CoRu)Ge was estimated as 7.5 K by magnetization, electrical resistivity, and heat-capacity measurements, which is considerably higher than the $T_{Curie} \sim 3$ K of the parent compound UCoGe [28]. In comparison with the tiny spontaneous magnetic moment of UCoGe, $0.07 \mu_B$/f.u., it was enhanced to $0.21 \mu_B$/f.u. in the case of U(CoRu)Ge for the c axis, the easy axis of magnetization of UCoGe and U(CoRu)Ge. The superconductivity was absent in U(CoRu)Ge [16,17,28]. YCoGe has a similar TiNiSi-type crystal structure to UCoGe as found in Fig. 1 in Ref. [30]. From the electric resistivity measurement in the single-crystal YCoGe, this compound is a typical metal with a small value of the electronic coefficient and has no magnetic and superconducting anomalies down to 0.3 K [30]. A polycrystal sample of hexagonal close-packed Co metal (Nilaco Corporation, Cobalt Rod 99.995%, CO-102598) was also used as one of the most typical references.

The XMCD experiments were carried out at the beamline BL23SU of SPring-8 [31]. For UCoGe and U(CoRu)Ge, we conducted the XMCD experiments at U-$N_{4,5}$, Co-$L_{2,3}$, and Ge-$L_{2,3}$. Mainly, we concentrated on the XMCD experiments at U-$N_{4,5}$ and Co-$L_{2,3}$ in order to grasp the magnetic information of the U $5f$ and Co $3d$ electrons separately. In addition, we performed the XMCD experiments at Co-$L_{2,3}$ on YCoGe and Co metal for comparison. Clean surfaces of single-crystal samples (polycrystal Co metal sample) were obtained by fracturing (by filing) in an ultrahigh vacuum just before the experiments. The temperature of samples was controlled by a combination of a liquid helium flow–type cryostat with an electrical heater. Since the lowest T was 5.5 K in the present study, the experiments on UCoGe were performed only in the PM state, while in the case of U(CoRu)Ge, both the PM and FM states were attainable. The external H was applied to the sample along the c axis using a superconducting magnet available up to 10 T. The experiment on YCoGe was also done under the $H \parallel c$ axis. The circularly polarized x rays were irradiated onto the sample along the axis of H. X-ray absorption spectra (XAS), defined as $\mu^+ + \mu^-$, were collected by the total electron yield method. The XMCD signals, defined as $\mu^+ - \mu^-$, were collected by switching the helicity

of light with 1 Hz at each photon energy using a twin-helical undulator of in-vacuum type [31]. Here, $\mu^+(\mu^-)$ refers to the x-ray absorption coefficient for the photon helicity parallel (antiparallel) to the majority-spin direction of respective electronic orbitals. The XMCD spectra shown in this paper were averaged by reversing H to cancel out artifacts caused by the asymmetry of the XMCD measurement system.

III. RESULTS

Figure 1(a) shows XAS spectra of UCoGe and U(CoRu)Ge at U-$N_{4,5}$ and Co-$L_{2,3}$ taken at $T = 5.5$ K and $H = 10$ T. The XAS spectra are normalized at U-N_5 ($h\nu = 734.9$ eV). Reflecting Ru doping, the absorption intensity at Co-$L_{2,3}$ becomes slightly smaller in U(CoRu)Ge than in UCoGe. Figure 1(b) shows XMCD spectra of UCoGe at $T = 5.5$ K and $H = 3$, 5, and 10 T. The most prominent peak of XAS and XMCD spectra around $h\nu = 776.4$ eV consists of two components coming from U-N_4 and Co-L_3, which overlap each other. Although UCoGe is in the PM state at $T = 5.5$ K, the XMCD signals are clearly detected. Compared with the overlapped XMCD peak at U-N_4 and Co-L_3, the XMCD intensities at U-N_5 and Co-L_2 are much smaller but can be observed clearly, as shown in the left and right insets of Fig. 1(b), respectively. This observation of the XMCD signals at U-N_5 is in distinct contrast with the previous soft x-ray XMCD experiment [24], in which the XMCD signals at U-N_5 have not been observed even in the FM state at $T = 2$ K. The XMCD spectra of U(CoRu)Ge are displayed in Fig. 1(c). In the case of U(CoRu)Ge, we were able to perform the XMCD experiments in both the PM and FM states, since the value of T_{Curie} had been pushed up to 7.5 K by the Ru substitution for Co [16,17,28]. The s shape of the XMCD spectra at U-N_5 is commonly observed in uranium compounds as shown in the left insets of Figs. 1(b) and 1(c), which is similar to the XMCD spectra at U-M_5 reported previously [25]. On the other hand, the shape of the XMCD spectrum of both UCoGe and U(CoRu)Ge at Co-L_2 is very peculiar, and its intensity is suppressed significantly as mentioned later. There are two structures around Co-L_2 mainly, which consist of negative (at $h\nu = 791.2$ eV) and positive (around $h\nu = 792.5$ eV) ones as shown in the right insets of Figs. 1(b) and 1(c). Furthermore, a closer look reveals that there are notable differences in the shape of the XMCD spectra at Co-L_2 between UCoGe and U(CoRu)Ge, as discussed later. We should point out here that the shape of the XMCD spectra of UCoGe at Co-$L_{2,3}$ which has been reported in the previous soft x-ray XMCD experiment [24] is remarkably different from the present result.

Figure 2(a) shows XAS spectra of UCoGe and U(CoRu)Ge at Ge-$L_{2,3}$ taken at $T = 5.5$ K and $H = 10$ T. The XAS spectra are normalized at $h\nu = 1225.4$ eV. The corresponding XMCD spectra are shown in Fig. 2(b). The XMCD intensity is based on the normalization of the XAS spectra in Fig. 2(a). In the region of Ge-$L_{2,3}$, the two transitions of $2p \rightarrow 4s$ and $2p \rightarrow 4d$ can be considered. Moreover, there is U-N_2 around $h\nu \sim 1271$ eV. Therefore it is difficult to discuss the electronic states at the Ge sites in detail without theoretical calculations. One can say safely that the XMCD signals are observed clearly at the Ge sites, and there is no difference between UCoGe and U(CoRu)Ge in these spectra within
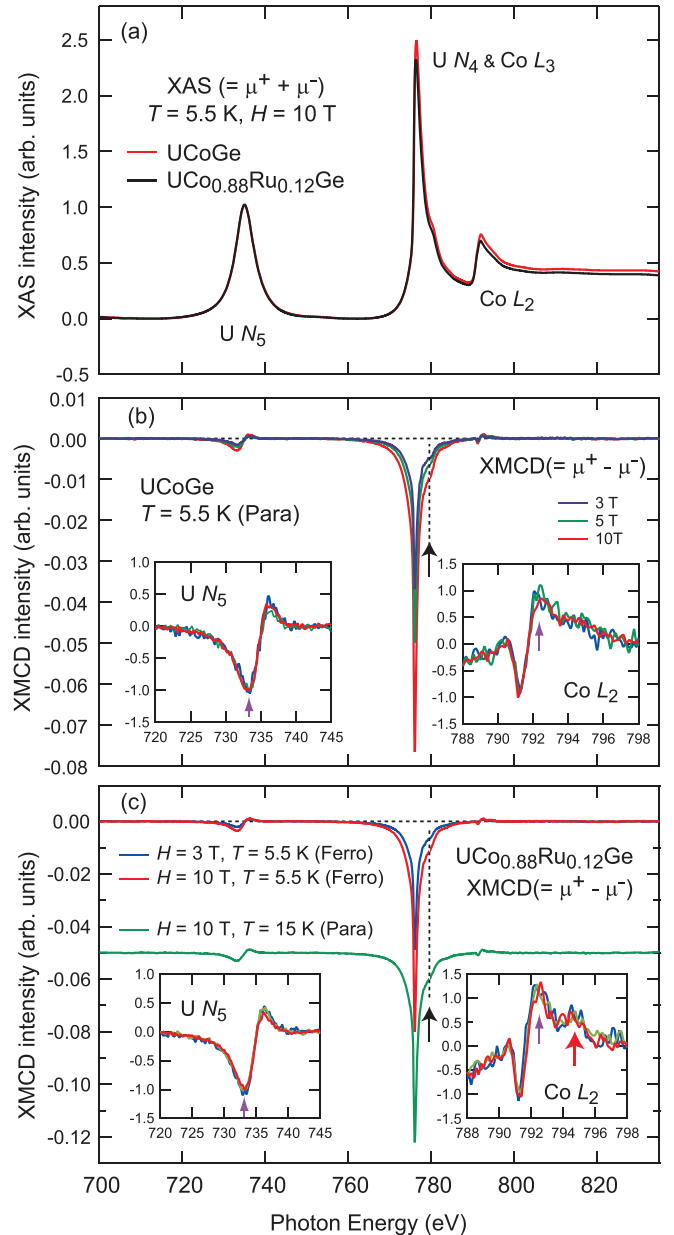

FIG. 1. Experimental XAS and XMCD spectra of UCoGe, U($\text{Co}_{0.88}\text{Ru}_{0.12}$)Ge. (a) XAS spectra of UCoGe and U($\text{Co}_{0.88}\text{Ru}_{0.12}$)Ge at U-$N_{4,5}$ and Co-$L_{2,3}$ measured at $T = 5.5$ K and $H = 10$ T. (b) XMCD spectra of UCoGe at $T = 5.5$ K and $H = 3$, 5, and 10 T. (c) XMCD spectra of U($\text{Co}_{0.88}\text{Ru}_{0.12}$)Ge. The upper spectra were measured at $T = 5.5$ K and $H = 3$ and 10 T. The lower spectrum was done at $T = 15$ K and $H = 10$ T. Right and left insets of panels (b) and (c) show enlarged plots at U-N_5 and Co-L_2, which are normalized to overlap each other, respectively. The purple arrows in the insets indicate the photon energy at which the XMCD-H curves were measured, as shown in Fig. 4. See text for the black arrows in panels (b) and (c), and the red arrow in the left inset of panel (c).

the experimental errors. The magnitudes of the respective XMCD intensities are comparable, even though UCoGe and U(CoRu)Ge are in the PM and FM states, respectively, at $T = 5.5$ K and $H = 10$ T. In addition, it is interesting that the shape
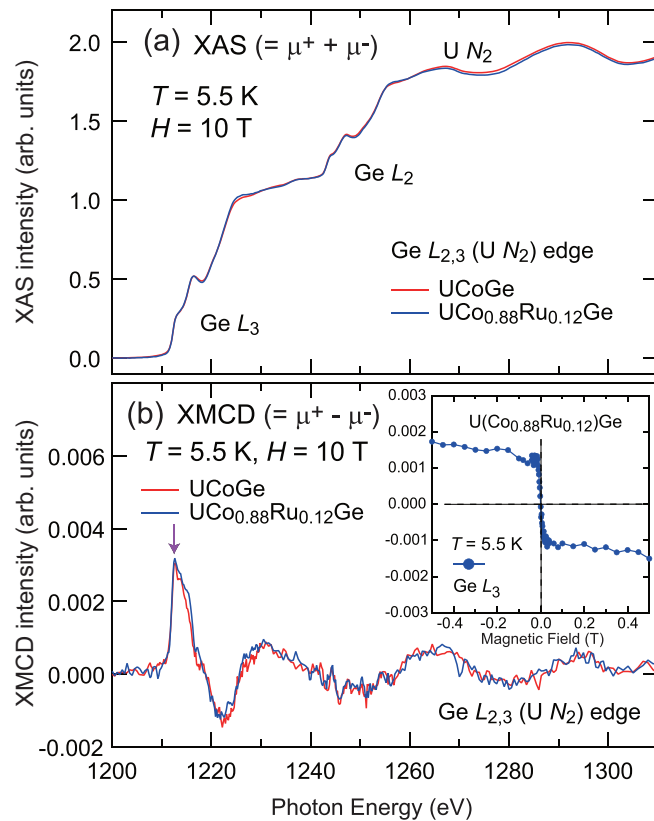
FIG. 2. Experimental XAS and XMCD spectra of UCoGe and U(CoRu)Ge at Ge-$L_{2,3}$ measured at $T = 5.5$ K and $H = 10$ T. (a) XAS spectra and (b) XMCD spectra. Inset shows the XMCD-H curve of U(CoRu)Ge at Ge-L_3 measured at $T = 5.5$ K. The purple arrow in panel (b) indicates the photon energy at which the XMCD-H curve was measured, as shown in the inset.

of the XMCD spectra of UCoGe and U(CoRu)Ge at Ge-$L_{2,3}$ are similar to that of UGe$_2$ [32,33]. Although there are very few reports about the XMCD spectrum at Ge-$L_{2,3}$, it is worth comparing with other materials such as the van der Waals magnet Fe$_5$GeTe$_2$ [34] and Heusler alloy Co$_2$MnGe [35], as discussed later. On the other hand, we could not detect the XMCD signals at Ru-$M_{2,3}$ within experimental accuracy. Even if the XMCD signals at Ru-$M_{2,3}$ exist, they would be much smaller than those at U-$N_{4,5}$, Co-$L_{2,3}$, and Ge-$L_{2,3}$ at most and do not contribute substantially to the total magnetism.

To examine the effects of the U 5f electrons on the electronic states of the Co 3d electrons in a material with the orthorhombic TiNiSi-type structure, we have chosen YCoGe as a reference compound without 5f electrons. Figures 3(a) and 3(b) show XAS and XMCD spectra of YCoGe at Co-$L_{2,3}$, respectively. The XMCD spectra are measured at $T = 10$ K and $H = 5$ and 10 T. Figures 3(c) and 3(d) show XAS and XMCD spectra of hexagonal close-packed Co metal, as another reference, at Co-$L_{2,3}$ taken at $T = 300$ K and $H = 2$ T. The normalization of these XAS spectra is done so that the XAS intensity at Co-L_3 becomes 1. The shapes of the XAS and XMCD spectra of YCoGe are independent of H. Compared with the XMCD intensity of UCoGe and U(CoRu)Ge, the XMCD intensity of YCoGe is one order of

magnitude smaller, reflecting that YCoGe is in the PM state with a small magnetic susceptibility [30], whereas, the XMCD intensity of Co metal is much larger than that of UCoGe, U(CoRu)Ge, and YCoGe. Figure 3(e) compares the XMCD spectrum of YCoGe ($T = 10$ K and $H = 10$ T) with the XMCD spectrum of Co metal ($T = 300$ K and $H = 2$ T). In general, the XMCD spectrum of Co compounds consists of two main peaks corresponding to Co-L_2 and Co-L_3 with comparable magnitudes and opposite signs as observed in the case of Co metal. Intriguingly, however, the XMCD spectrum of YCoGe has a much smaller intensity at Co-L_2 than that at Co-L_3, and the shape of the XMCD spectrum of YCoGe at Co-L_2 is quite different from that of Co metal as displayed in the inset of Fig. 3(e). The similar feature in the XMCD spectra at Co-L_2 is also observed in UCoGe and U(CoRu)Ge, as shown in the right insets of Figs. 1(b) and 1(c). Furthermore, there is a shoulder structure in the XAS and XMCD spectra marked by the black arrow at $h\nu = 779$ eV in Figs. 3(a) and 3(b). This indicates that the shoulder structures in the XAS and XMCD spectra of UCoGe and U(CoRu)Ge observed at the same photon energy are also ascribed to the electronic states of the Co 3d electrons, as indicated by the black arrows and vertical dotted lines in Figs. 1(b) and 1(c). This is a reasonable conclusion because the XMCD spectrum at U-N_4, like that at U-M_4, usually shows a symmetric shape with no fine structures. Indeed, the symmetric shape of the XMCD spectrum of UCoGe has been observed at U-M_4 in hard x-ray XMCD experiment [25].

In order to obtain element-specific magnetization curves, the H dependence of the XMCD intensity (XMCD-H curve) of UCoGe and U(CoRu)Ge is measured at U-N_5 ($h\nu = 733.3$ eV), Co-L_2 ($h\nu = 792.5$ eV), while the Co-L_3 ($h\nu = 776.0$ eV) is used for YCoGe. The XMCD-H curve of YCoGe has a linear dependence on H, clearly indicating that this is a paramagnet as shown in the inset of Fig. 3(b). Indeed, there is no magnetic anomaly in the electric resistivity and specific-heat measurements on YCoGe [30]. The ^{59}Co NQR and NMR experiments have revealed that YCoGe is in a conventional metallic state without notable magnetic fluctuations down to 1.5 K [30]. For UCoGe, the XMCD-H curves recorded from 5.5 to 50 K are displayed in Figs. 4(a) and 4(b) at the U and Co sites, respectively. At $T = 50$ K, the XMCD-H curves show almost linear H dependence at both the U and Co sites. As T decreases, the XMCD intensity increases and the XMCD-H curve gradually changes to a curved shape. This implies that the FM behavior develops drastically at the low-T range, especially below 10 K, even in the PM state. Note that the XMCD-H curve begins to bend more convexly at the U site than at the Co site, as shown in Figs. 4(a) and 4(b). Meanwhile, the XMCD-H curves of U(CoRu)Ge at the U and Co site are shown in Figs. 4(c) and 4(d), respectively. The XMCD-H curves are measured at $T = 5.5$ and 15 K, below and above T_{Curie}. The insets of Figs. 4(c) and 4(d) show the enlarged plots in the range of $H = \pm 0.5$ T. The XMCD-H curves have opposite signs, because the XMCD signals at U-N_5 and Co-L_2 are negative and positive signs, respectively, as denoted by purple arrows in the insets of Figs. 1(b) and 1(c). The FM transition is clearly detected as a steep jump of the XMCD-H curves at $T = 5.5$ K around $H = 0$ T, as reported from the bulk magnetization
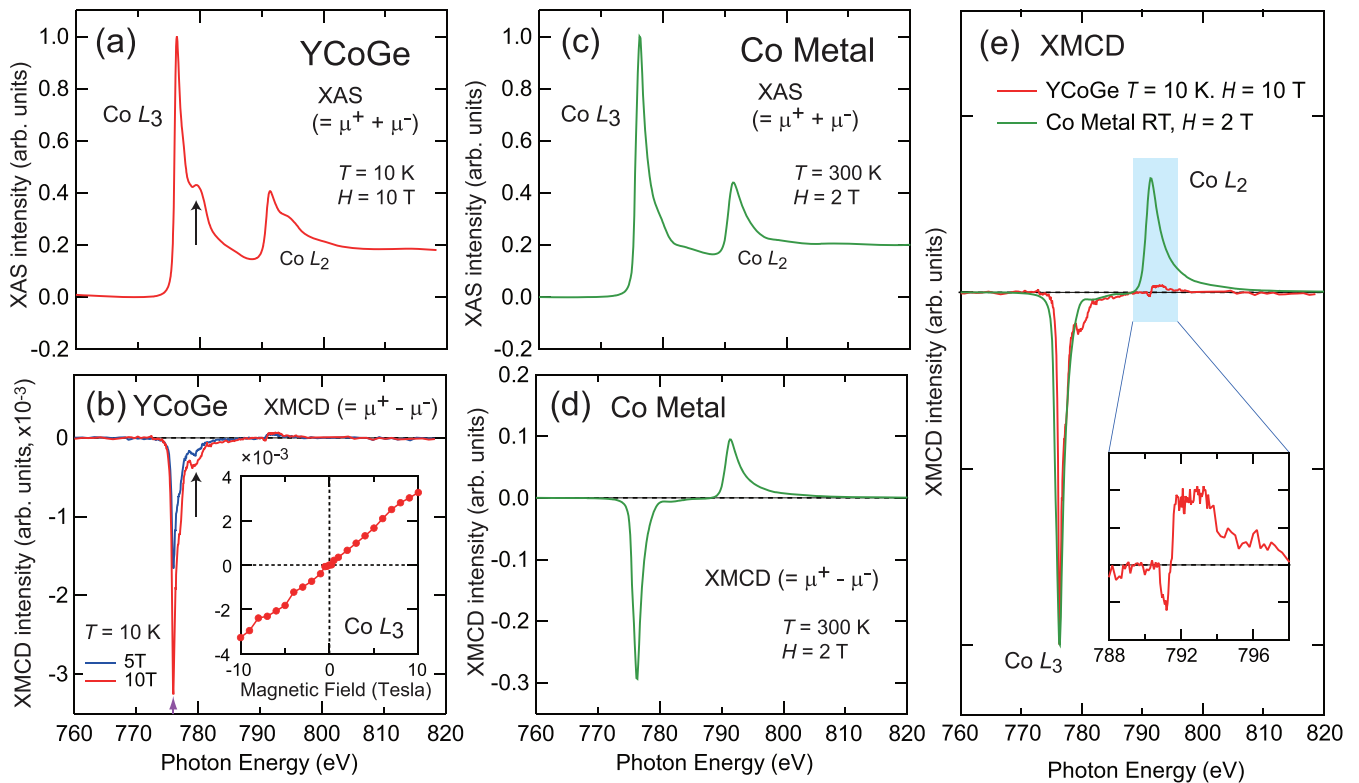
FIG. 3. Experimental XAS and XMCD spectra of YCoGe, and comparison of XMCD spectra of YCoGe and Co metal. (a) XAS spectrum of YCoGe at Co-$L_{2,3}$ measured at $T = 10$ K and $H = 10$ T. (b) XMCD spectra of YCoGe at $T = 10$ K and $H = 5$ and 10 T. Inset shows the XMCD-H curve at Co-L_3 (indicated by the purple arrow) measured at $T = 10$ K. (c) XAS spectrum of Co metal at Co-$L_{2,3}$ measured at $T = 300$ K (RT) and $H = 2$ T. (d) XMCD spectrum of Co metal at RT and $H = 2$ T. (e) Comparison of XMCD spectra of YCoGe and Co metal. The width of the XMCD spectrum of YCoGe at Co-L_3 is narrower than that of Co metal. Inset shows enlarged spectra of YCoGe around Co-L_2.

measurement [16,28]. In addition, as shown in the inset of Fig. 2(b), the clear step is observed in the XMCD-H curve taken at Ge-L_3 at $h\nu = 1212.6$ eV (marked by the purple arrow), suggesting that the magnetic polarization exists at the Ge site.

Figure 5(a) shows the T dependence of the XMCD intensity of UCoGe at $H = 2$, 5, and 10 T, which are extracted from the XMCD-H curves in Figs. 4(a) and 4(b). Each plot represents the XMCD intensity divided by the corresponding H strength (XMCD/H), in other words, the slope of the XMCD-H curve at the measured H from $H = 0$ T. The left (for U-N_5 edge) and right (for Co-L_2) vertical axes are adjusted so that the values at $T = 50$ K overlap within the experimental errors. In the range between $T = 40$ and 50 K, the value of XMCD/H at every H point is almost the same, meaning that the XMCD-H curve is linear with respect to H strength in the high-T range. As T decreases, the difference in the XMCD/H between the U and Co sites becomes more significant at the lower H range and the T dependence at the U site is much stronger than at the Co site. This behavior is ascribed to the curved shape of the XMCD-H curves in the low-T range, as pointed out in Figs. 4(a) and 4(b). Meanwhile, in the case of U(CoRu)Ge, the XMCD-H curves are displayed again in Fig. 5(b). The normalization of the XMCD-H curves is done by adjusting ranges of the left (for U-N_5 edge) and right (for Co-L_2) vertical axes so that the XMCD-H curves of the U and Co sites at $T = 15$ K overlap each other. Unlike

UCoGe, overall, the increase of the XMCD intensity at the U site shows a similar tendency to that at the Co site on cooling from 15 to 5.5 K. However, concerning the jump of the XMCD-H curve at around $H = 0$ T, it becomes steeper at the Co site than at the U site at $T = 5.5$ K.

Next, to see the effect of Ru substitution on the XMCD-H curves, the XMCD-H curves of UCoGe and U(CoRu)Ge are compared at $T = 5.5$ K. Figures 5(c) and 5(d) show the XMCD-H curves at the U and Co sites, respectively. Since U(CoRu)Ge is in the FM state and UCoGe is in the PM state at $T = 5.5$ K, overall the XMCD intensity of U(CoRu)Ge is larger than that of UCoGe, as shown in Figs. 4(a)–4(d). For comparison of the shape of the XMCD-H curves, the XMCD-H curves are normalized by adjusting the range of the left, for UCoGe, and right, for U(CoRu)Ge, vertical axes so that they overlap each other. In the high-H range, the shapes of XMCD-H curves at both sites coincide well, whereas in the low-H range, especially around $H = 0$ T, the jump of the XMCD-H at the Co site is remarkable compared with that at the U site. This comparison reveals that the Ru substitution affects the XMCD-H curves much more significantly at the Co site than at the U site.

IV. DISCUSSIONS

In the present soft x-ray XMCD study, we have captured the XMCD signals at both the U and Co sites in UCoGe
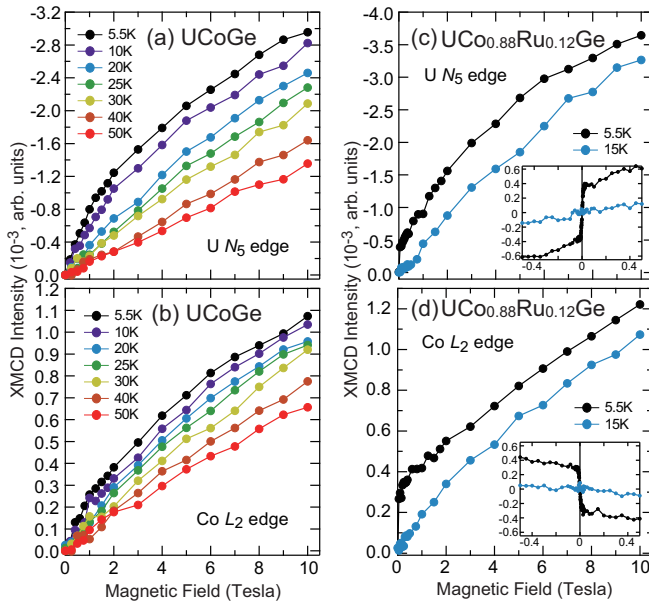
FIG. 4. *H* dependence of the XMCD intensity (XMCD-*H* curve) at several *T*s. Panels (a) and (b) show XMCD-*H* curves of UCoGe at U-N_5 and Co-L_2, respectively. These are measured at $T = 5.5$, 10, 20, 25, 30, 40, and 50 K. Panels (c) and (d) show XMCD-*H* curves of U(Co$_{0.88}$Ru$_{0.12}$)Ge at U-N_5 and Co-L_2 edge, respectively. These are measured at $T = 5.5$ and 15 K. In the insets, the enlarged XMCD-*H* curves in the range $H = \pm 0.5$T are shown.

and U(CoRu)Ge, unlike the previous soft x-ray XMCD experiment [24]. Thus we can extract information about the orientation of the magnetic moments of U $5f$ and Co $3d$ electrons simultaneously. Firstly, we have found that the shape of the XMCD spectra at U-N_5 is identical to that at U-M_5, and the sign of the XMCD intensity at U-N_4 is distinctly negative, as shown in Fig. 1. According to the sum rules for the XMCD spectra [36,37] which can determine the direction and magnitude of the spin magnetic moment (M_S) and M_L element specifically, the main coefficients in the formulas can be decided by the azimuthal quantum numbers of the electron orbitals of ground-state core and excited-state valence electrons. Since the coefficients are the same in the case of U-$N_{4,5}$ and U-$M_{4,5}$, in principle, equivalent information about the magnetic moment of the U $5f$ electrons should be obtained at these two absorption edges. In the previous XMCD experiments at U-$M_{4,5}$, detailed analysis by the sum rules has shown that the M_L oriented parallel to the applied *H* direction is larger than the M_S oriented antiparallel to it [25]. Thus it is convincing that the total magnetic moment of the $5f$ electrons in UCoGe and U(CoRu)Ge are parallel to the applied *H* direction under all the experimental conditions in the present study. Meanwhile, in the case of the hard x-ray XMCD experiment, it is difficult to extract the magnetic information of the Co $3d$ electrons directly.

Next we discuss the direction of the magnetic moment of the Co $3d$ electrons. According to the sum rules [36,37] for the $3d$ TM $L_{2,3}$ edge, the equations for the quantitative estimation of M_S and M_L are written by

$$M_S = -2 < S_Z > = -\frac{6p - 4q}{r} n_h + 7 < T_Z >, \quad (1)$$
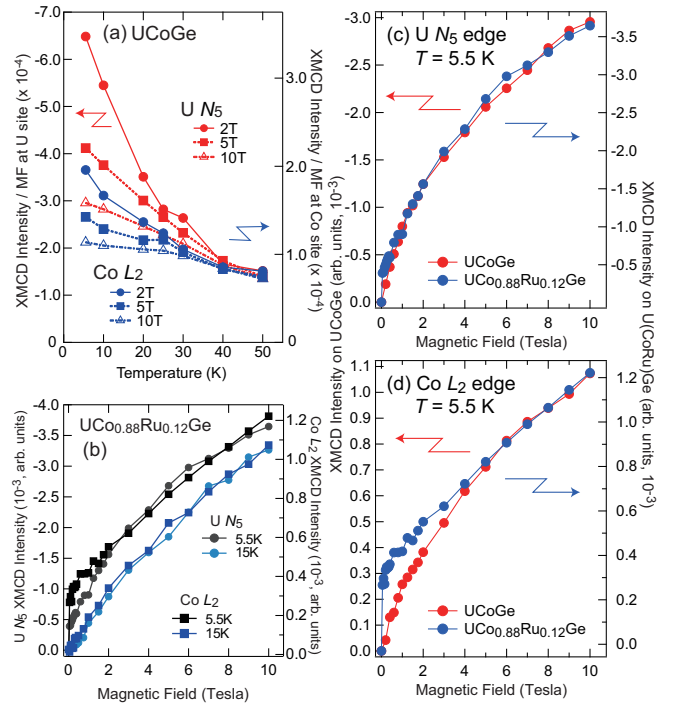

FIG. 5. Comparison of magnetic properties of UCoGe and U(Co$_{0.88}$Ru$_{0.12}$)Ge. (a) The *T* dependence of XMCD intensity divided by *H* strength (XMCD/*H*) of UCoGe at $H = 2$, 5, and 10 T. (b) The *T* dependence of the XMCD-*H* curves of U(Co$_{0.88}$Ru$_{0.12}$)Ge. (c, d) The comparison of the XMCD-*H* curves of UCoGe and U(Co$_{0.88}$Ru$_{0.12}$)Ge at $T = 5.5$ K. Panels (c, d) are the comparison at the U N_5 and Co L_2 edges, respectively. In these panels, the normalization is done by adjusting the ranges of the left and right vertical axes (see text).

$$M_L = - < L_Z > = -\frac{4q}{3r} n_h, \quad (2)$$

where $< S_Z >$, $< T_Z >$, and $< L_Z >$ are the expectation values of the *z* component of the spin angular momentum, the magnetic dipole operator, and the orbital angular momentum, respectively. In addition, n_h is the number of unoccupied $3d$ holes, p (q) is the integral of the XMCD spectrum over TM-L_3 (TM-$L_{2,3}$), and r is the integral of the XAS spectrum over TM-$L_{2,3}$. Unfortunately, it is difficult to guarantee the reliability of the quantitative estimation of the magnetic moments, since there are several assumptions and unknown terms which cause serious errors when the sum rules are applied for the case of UCoGe and U(CoRu)Ge, for example, due to the overlapping of U-N_4 and Co-L_3 in XAS and XMCD spectra. However, we can draw insight into the direction of the magnetic moment of the Co $3d$ electrons as explained below.

Figure 6(a) shows the integrals of the XMCD spectra of UCoGe, U(CoRu)Ge, and YCoGe. In principle, the information about the U $5f$ electrons obtained from the XMCD spectra at U-$N_{4,5}$ should be identical to that obtained at U-$M_{4,5}$ from the hard x-ray XMCD experiment [25], as aforementioned. Using the results at U-$M_{4,5}$, we have estimated the ratio of the integral over U-M_4 (hereafter denoted as U-M_4 integral) to U-M_5 integral, and have obtained that the
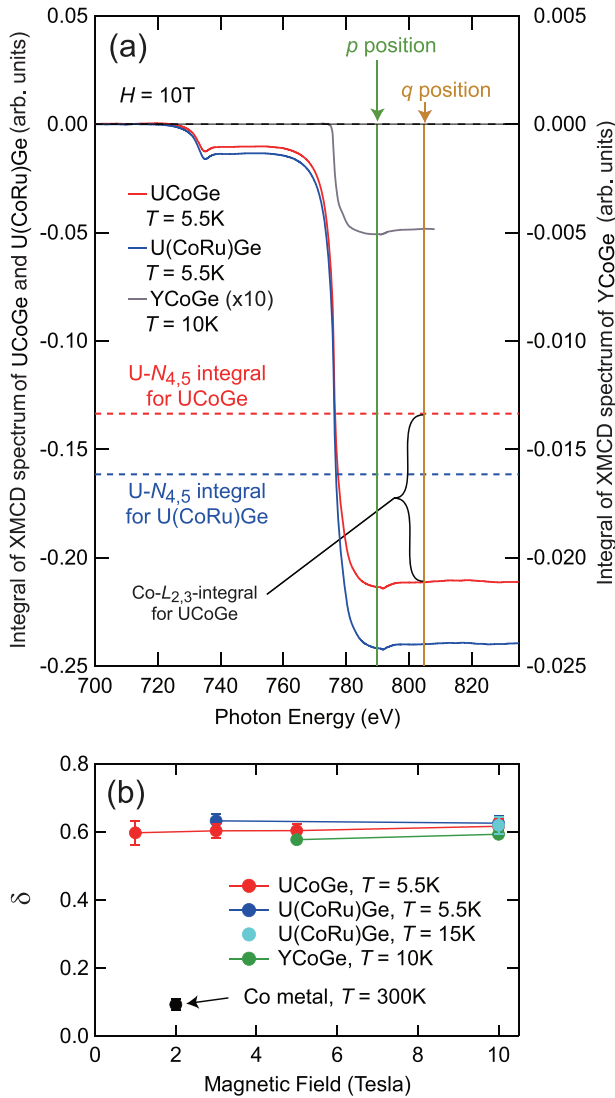
FIG. 6. Analysis using the sum rules [36,37] at Co-$L_{2,3}$. (a) Integrals of the XMCD spectra of UCoGe ($T = 5.5$ K, $H = 10$ T), U(Co$_{0.88}$Ru$_{0.12}$)Ge ($T = 5.5$ K, $H = 10$ T), YCoGe ($T = 10$ K, $H = 10$ T). The integral of YCoGe is multiplied by 10, displayed in the right vertical axis. The red and blue horizontal dotted lines show the U-$N_{4,5}$ integral of UCoGe and U(Co$_{0.88}$Ru$_{0.12}$)Ge, respectively, deduced from the result of the XMCD spectrum at U-$M_{4,5}$ [25] (see text). The green (brown) vertical line and arrow show the photon energy position where p, the Co-L_3 integral (q, Co-$L_{2,3}$ integral) is taken. For example, the q value (Co-$L_{2,3}$ integral) is obtained as displayed with a black close brace. (b) T and H dependence of the values of δ for UCoGe, U(Co$_{0.88}$Ru$_{0.12}$)Ge, YCoGe, and Co metal.

U-M_4 integral is 11.03 times larger than the U-M_5 integral at $T = 2.1$ K and $H \parallel c$ axis $= 17$ T. We have made a rough assumption that this ratio of the integral is not changed significantly in the present XMCD spectra of UCoGe and U(CoRu)Ge, although the experimental conditions are different. Under the above assumption, we have deduced the U-$N_{4,5}$ integral so that it satisfies the ratio of the integral at U-$M_{4,5}$. The red (blue) horizontal dotted line in Fig. 6(a) is the deduced U-$N_{4,5}$ integral of UCoGe [U(CoRu)Ge], which is obtained

by adding U-N_5 integral to the value that is multiplied U-N_5 integral by 11.03 (namely, U-$N_{4,5}$ integral $=$ U-N_5 integral $\times$ $(1 + 11.03)$). By subtracting the deduced U-$N_{4,5}$ integral from the total integral over U-$N_{4,5}$ and Co-$L_{2,3}$, the integrals p and q only for Co-$L_{2,3}$ can be obtained. For example, the q value (Co-$L_{2,3}$ integral) for UCoGe is obtained as displayed with a black close brace in Fig. 6(a). Using the p and q values, we can determine the direction of the magnetic moment of the Co 3d electrons just by checking the signs of Eqs. (1) and (2). Both positive values obtained from the two equations, assuming the value of $\langle T_Z \rangle$ is small for TMs as usual, conclude that both the M_S and M_L of the Co 3d electrons are oriented to the applied H direction. Therefore both the total magnetic moments of the U 5f and Co 3d electrons are parallel to the H direction. This relation of the magnetic moments of the U 5f and Co 3d electrons in UCoGe and U(CoRu)Ge is the same analogy as that found in UCoAl [38,39]. It should be noted that the orientation of the magnetic moments of the U 5f and Co 3d electrons is not changed above and below T_{Curie} in the case of U(CoRu)Ge, consistent with the results obtained by the PND experiment on U(CoRu)Ge [28]. If the flip of the magnetic moment at the Co site occurs in UCoGe according to the suggested result by PND [23], the XMCD intensity around $h\nu = 776.4$ eV would be drastically suppressed, and/or the sign changes from negative to positive. In practice, we have found that the XMCD intensities at the U and Co sites continue to increase monotonously as T decreases, at least down to 5.5 K, and there is no indication of flipping the sign of the XMCD intensity at Co-$L_{2,3}$. It should be noted again that such a flip does not occur when U(CoRu)Ge becomes from the PM to the FM states. The precise soft x-ray XMCD experiment on UCoGe below T_{Curie} is highly desired.

We can deduce the direction of the magnetic moment at the Ge site from the XMCD spectra of other compounds at Ge-$L_{2,3}$. In the case of UCoGe, U(CoRu)Ge (and including UGe$_2$ [32]), the two peaks of the XMCD spectra at Ge-L_3 have positive (at 1212.6 eV) and negative (at 1222.2 eV) signs, as shown in Fig. 2(b), whereas these signs are opposite in the case of Fe$_5$GeTe$_2$ [34] and Co$_2$MnGe [35]. It has been concluded that the direction of the magnetic moment at the Ge site is antiparallel to the applied H direction in Fe$_5$GeTe$_2$[34] and Co$_2$MnGe [35,40]. Therefore it is deduced that the magnetic moment at the Ge site is parallel to the applied H direction in UCoGe and U(CoRu)Ge, meaning that magnetic moments at the U, Co, and Ge sites are aligned in the same direction.

From Eqs. (1) and (2), the following ratio is obtained:

$$\delta = \frac{< L_Z >}{2 < S_Z > + 7 < T_Z >} = \frac{2q}{9p - 6q}. \tag{3}$$

The ratio δ is independent of n_h and r, and can be estimated by the two integrals p and q, obtained only from the XMCD spectrum. Although $< T_Z >$ cannot be known experimentally, δ can be roughly regarded as the ratio M_L/M_S and is useful to characterize the electronic and magnetic properties of 3d electrons of a target TM. Therefore it is worthwhile to compare the δ among UCoGe, U(CoRu)Ge, and YCoGe for understanding the electronic states of the Co 3d electrons in the material with the TiNiSi-type orthorhombic structure. Figure 6(b) shows the δ obtained by using Eq. (3) for the XMCD spectra of UCoGe [Fig. 1(b)], U(CoRu)Ge [Fig. 1(c)], YCoGe [Fig. 3(b)], and

Co metal [Fig. 3(d)]. When we apply Eq. (3) for UCoGe and U(CoRu)Ge, the same ratio (U-N_4 integral/U-N_5 integral) deduced from the XMCD experiment at U-$M_{4,5}$ is used as shown in Fig. 6(a). The $\delta \sim 0.09$ for Co metal is consistent with the result reported by the XMCD experiment in the early days [41], indicating that M_L is remarkably quenched. On the other hand, the δ for UCoGe, U(CoRu)Ge, and YCoGe is ~ 0.6 under all the present experimental conditions and is much larger than that for Co metal. The notable result is ascribed to the peculiar shape of the XMCD spectrum at Co-L_2 as aforementioned. This leads to a large residual negative q value. It should be emphasized here that even YCoGe without the U $5f$ electrons has the large δ, as do UCoGe and U(CoRu)Ge. This suggests that the peculiar shape of the XMCD spectra at Co-$L_{2,3}$ is not due to the hybridization of U $5f$ and Co $3d$ electrons but to the TiNiSi-type orthorhombic structure.

It is worth noting that the shape of the XMCD spectrum at Co-$L_{2,3}$ is very similar to that observed in the system where atomic Co forms clusters on potassium in Fig. 3 of Ref. [42]. At low Co coverage, the XMCD intensity at Co-L_2 has a negative sign, i.e., the same sign as the intensity at Co-L_3, resulting in a larger δ of about 0.9. As the Co cluster size increases, δ decreases and eventually reaches ~ 0.1, similar to bulk Co metal. At intermediate Co coverage where δ becomes ~ 0.6, the shape of the XMCD spectra resembles the observed ones in this study. The surprising similarity to the atomiclike system implies that the Co $3d$ electrons in these compounds are in a low-symmetry electronic environment even in solid states and/or hybridize anisotropically with other electrons. As shown in Fig. 3(e), the width of the XMCD spectrum of YCoGe at Co-L_3 is narrower than that of Co metal, indicative of the localized character of the Co $3d$ electrons. As another example that demonstrates the correlation between a low-symmetry system and large M_L, in the low-symmetry triclinic phase of van der Waals FM VI$_3$, unquenched M_L at the vanadium site was very recently detected [43].

Interestingly, in another FM SC URhGe with the same crystal structure, a large $\delta \sim 0.67$ was found from the XMCD spectrum at Rh-$L_{2,3}$ ($2p \rightarrow 4d$) since no XMCD signal is detected at Rh-L_2 [44]. In addition, the XMCD intensity at Ge-L_2 of the U-based FM SCs is significantly suppressed compared to that of Fe$_5$GeTe$_2$ [34] and Co$_2$MnGe [35]. Probably, the suppression of the XMCD intensity at Ge-L_2 is also related to the above-mentioned situation about the Co $3d$ electrons, because the Co and Ge atoms form the alternative chain structure in the orthorhombic TiNiSi-type structure. Thus we deduce that this crystal structure is a unique platform for realizing the variety of physical properties that appear in FM SCs.

Here we note that the differences in the shape of the XMCD spectra at Co-L_2 are detected among YCoGe, UCoGe, and U(CoRu)Ge, although overall the shapes are similar. The single negative peak at $h\nu = 791.2$ eV is observed commonly among the three compounds. Concerning the positive peaks above $h\nu = 792$ eV, the structure at $h\nu = 793.0$ eV is broad or seems to consist of some peaks in YCoGe, as shown in the inset of Fig. 3(e). In UCoGe, as shown in the right inset of Fig. 1(b), the peak at $h\nu = 792.5$ eV becomes more distinct than in YCoGe. Indeed, it has been reported that the XMCD spectral shape of UCoGe at Co-K is also different from that of YCoGe [25], meaning that the U $5f$ electrons

affect the electronic states at the Co site. Furthermore, by the Ru substitution for Co, the shape of the XMCD spectra of U(CoRu)Ge becomes sharper than that of UCoGe. For example, when the amplitude of the negative peak at $h\nu = 791.2$ eV is normalized to 1, it can be noticed that the positive peak at $h\nu = 792.5$ eV is enhanced in U(CoRU)Ge compared with the case of UCoGe, and the structure at $h\nu = 795$ eV develops in U(CoRu)Ge as highlighted by the red arrow in the right inset of Fig. 1(c). Therefore it is considered that the Co $3d$ electrons are modified due to the presence of the U $5f$ electrons and the Ru substitution. On the other hand, no change in the XMCD spectra at U-N_5 [the left insets of Figs. 1(b) and 1(c)] and Ge-$L_{2,3}$ [Fig. 2] can be observed between UCoGe and U(CoRu)Ge within the present experimental accuracy.

Next we focus on the development of the FM ordering based on the element-specific magnetization curves, i.e., XMCD-H curves. From the comparison between YCoGe and UCoGe, it is clear that the presence of the U $5f$ electrons remarkably enhances the magnetic susceptibility and strengthens the FM interaction, which is consistent with the results revealed by the ^{59}Co NQR and NMR experiments [30]. As T decreases, the XMCD intensity develops more strongly at the U site than at the Co site, as shown in Fig. 5(a). The difference in the increase of the XMCD intensity between the U and Co sites becomes significant at the lower H range. Although the XMCD experiment is a static magnetic probe, the remarkable enhancement of the XMCD intensity at the U site compared to that at the Co site might occur to the site-selective development of the FM fluctuations, which could correspond to the Ising-type FM fluctuations along the c axis growing especially below 10 K as reported from the ^{59}Co NMR experiments [8].

On the other hand, concerning the effects on the FM ordering by the Ru substitution, the shape of the XMCD-H curve at the Co site becomes more rectangular than that at the U site below T_{Curie} as shown in Fig. 5(b). Furthermore, from the comparison between UCoGe and U(CoRu)Ge in Figs. 5(c) and 5(d), it is found that the Ru substitution affects the shape of the XMCD-H curve at the Co site more significantly than at the U site. As pointed out from the change in the shape of the XMCD spectra at Co-L_2 by the Ru substitution, it is natural to interpret that the change in the electronic state of the Co $3d$ electrons causes the drastic change in the XMCD-H curves at the Co site. According to the Co $2p$-$3d$ resonant photoemission spectroscopy, the Co $3d$ electrons in UCoGe have the finite density of states (DOS) at Fermi level (E_F) and hybridize with the U $5f$ electrons [45]. In addition, the electronic states are considered to be very sensitive to chemical substitution in the Co-Ge chains as observed in the changes of the XMCD spectra at Co-L_2. Therefore the Ru substitution could cause a remarkable modification of the Co $3d$ electronic states, which leads to changes of the DOS at E_F through the delicate balance of the hybridization of the U $5f$ and TM (Co and Ru) d electrons, as discussed by the theoretical model [46].

The separation of the magnetic behavior of the U $5f$ and Co $3d$ electrons reveals that the magnetism of the Co $3d$ electrons is not merely passively induced by the magnetism of the U $5f$ electrons but rather actively contributes to the stabilization of ferromagnetism in this system. This study

demonstrates clearly that the contribution of not only the U $5f$ electrons but also the TM d electrons is very important to disentangle the complicated physical properties of the FM SCs. We hope that the precise soft x-ray XMCD experiments in the FM state of UCoGe will be revisited and that theoretical advances focusing on the electronic states of the ligand atoms will be realized.

V. CONCLUSION

We investigated the element-specific electronic states and magnetic properties in UCoGe using the soft x-ray XMCD experiments at U-$N_{4,5}$, Co-$L_{2,3}$, and Ge-$L_{2,3}$. In addition, U(Co$_{0.88}$Ru$_{0.12}$)Ge, which has higher T_{Curie} but does not show superconductivity, was also studied to examine how the ferromagnetism of the system is stabilized by the Ru substitution for Co atoms. Moreover, we compared them with the XMCD spectrum at Co-$L_{2,3}$ of YCoGe, which has an identical crystal structure to UCoGe without the $5f$ electrons. From the obtained XMCD spectra, the magnetic moments of the U $5f$ and Co $3d$ electrons align in the same direction and are parallel to the applied H direction. Furthermore, it is deduced that the magnetic moment at the Ge site is also parallel to H from a comparison with the XMCD spectra at Ge-$L_{2,3}$ of other Ge-contained ferromagnetic materials. The shapes of the XMCD spectra of UCoGe at U-N_5 and Ge-$L_{2,3}$ are indistinguishably similar to those of U(Co$_{0.88}$Ru$_{0.12}$)Ge, whereas we found the XMCD spectra at Co-L_2 are very peculiar in UCoGe, U(Co$_{0.88}$Ru$_{0.12}$)Ge, and even in YCoGe. From the analysis using the sum rules for the XMCD spectra at Co-$L_{2,3}$, it is found that the Co $3d$ electrons have a very large orbital magnetic moment, suggesting that the Co $3d$ electrons are in a low-symmetry electronic environment. Moreover, the XMCD spectral shape at Co-L_2 depends on the compounds, meaning that the electronic states of the $3d$ electrons in this system could be very sensitive to the presence of the U $5f$ electrons and by the Ru substitution.

From the T and H dependence of XMCD intensity at U-N_5 and Co-L_2, we extracted the element-specific magnetic behavior at the U and Co sites. In UCoGe, as T decreases, the XMCD intensity at the U site is significantly enhanced, especially at the low-H range, compared with that at the Co site. This behavior could be an indication of the development of ferromagnetic fluctuations at the U site. In U(Co$_{0.88}$Ru$_{0.12}$)Ge, the XMCD intensities at the U and Co sites increase to a similar degree above $H \sim 2$ T as T decreases from 15 to 5.5 K, but the XMCD-H curve at the Co site around $H = 0$ T becomes steeper than that at the U site at $T = 5.5$ K. Furthermore, the comparison of the XMCD-H curves between UCoGe and U(Co$_{0.88}$Ru$_{0.12}$)Ge reveals that the ferromagnetic behavior of the XMCD-H develops much more strongly at the Co site than at the U site. Therefore we suggest the following mechanism for the stabilization of the ferromagnetism in this system: When the Co $3d$ electrons are on the verge of the ferromagnetic state, the element-selective ferromagnetic fluctuations of the U $5f$ electrons could be developed instead. On the other hand, when the Co $3d$ electrons prefer the ferromagnetic state at a relatively high temperature, the ferromagnetism in this system is stabilized, while superconductivity mediated by the ferromagnetic fluctuations of the U $5f$ electrons is significantly suppressed.

[1] S. S. Saxena, P. Agarwal, K. Ahilan, F. M. Grosche, R. K. W. Haselwimmer, M. J. Steiner, E. Pugh, I. R. Walker, S. R. Julian, P. Monthoux, G. G. Lonzarich, A. Huxley, I. Sheikin, D. Braithwaite, and J. Flouquet, Nature (London) **406**, 587 (2000).

[2] A. Huxley, I. Sheikin, E. Ressouche, N. Kernavanois, D. Braithwaite, R. Calemczuk, and J. Flouquet, Phys. Rev. B **63**, 144519 (2001).

[3] D. Aoki, A. Huxley, E. Ressouche, D. Braithwaite, J. Flouquet, J.-P. Brison, E. Lhotel, and C. Paulsen, Nature (London) **413**, 613 (2001).

[4] N. T. Huy, A. Gasparini, D. E. de Nijs, Y. Huang, J. C. P. Klaasse, T. Gortenmulder, A. de Visser, A. Hamann, T. Görlach, and H. v. Löhneysen, Phys. Rev. Lett. **99**, 067006 (2007).

[5] D. Aoki and J. Flouquet, J. Phys. Soc. Jpn. **83**, 061011 (2014).

[6] D. Aoki, K. Ishida, and J. Flouquet, J. Phys. Soc. Jpn. **88**, 022001 (2019).

[7] T. Ohta, T. Hattori, K. Ishida, Y. Nakai, E. Osaki, K. Deguchi, N. K. Sato, and I. Satoh, J. Phys. Soc. Jpn. **79**, 023707 (2010).

[8] Y. Ihara, T. Hattori, K. Ishida, Y. Nakai, E. Osaki, K. Deguchi, N. K. Sato, and I. Satoh, Phys. Rev. Lett. **105**, 206403 (2010).

[9] T. Hattori, Y. Ihara, Y. Nakai, K. Ishida, Y. Tada, S. Fujimoto, N. Kawakami, E. Osaki, K. Deguchi, N. K. Sato, and I. Satoh, Phys. Rev. Lett. **108**, 066403 (2012).

[10] T. Hattori, Y. Ihara, K. Karube, D. Sugimoto, K. Ishida, K. Deguchi, N. K. Sato, and T. Yamamura, J. Phys. Soc. Jpn. **83**, 061012 (2014).

[11] T. Hattori, K. Karube, K. Ishida, K. Deguchi, N. K. Sato, and T. Yamamura, J. Phys. Soc. Jpn. **83**, 073708 (2014).

[12] S. Ran, C. Eckberg, Q.-P. Ding, Y. Furukawa, T. Metz, S. R. Saha, I.-L. Liu, M. Zic, H. Kim, J. Paglione, and N. P. Butch, Science **365**, 684 (2019).

[13] D. Aoki, J.-P. Brison, J. Flouquet, K. Ishida, G. Knebel, Y. Tokunaga, and Y. Yanase, J. Phys.: Condens. Matter **34**, 243002 (2022).

[14] K. Huang, J. J. Hamlin, R. E. Baumbach, M. Janoschek, N. Kanchanavatee, D. A. Zocco, F. Ronning, and M. B. Maple, Phys. Rev. B **87**, 054513 (2013).

[15] J. Pospíšil, J. P. Vejpravová, M. Diviš, and V. Sechovský, J. Appl. Phys. **105**, 07E114 (2009).

[16] M. Vališka, P. Opletal, J. Pospíšil, J. Prokleška, and V. Sechovský, Adv. Nat. Sci: Nanosci. Nanotechnol. **6**, 015017 (2015).

[17] M. Vališka, J. Pospíšil, M. Diviš, J. Prokleška, V. Sechovský, and M. M. Abd-Elmeguid, Phys. Rev. B **92**, 045114 (2015).

[18] S. Sakarya, N. T. Huy, N. H. van Dijk, A. de Visser, M. Wagemaker, A. C. Moleman, T. J. Gortenmulder, J. C. P. Klaasse, M. Uhlarz, and H. v. Löhneysen, J. Alloys Compd. **457**, 51 (2008).

[19] J. Pospíšil, Y. Haga, S. Kambe, Y. Tokunaga, N. Tateiwa, D. Aoki, F. Honda, A. Nakamura, Y. Homma, E. Yamamoto, and T. Yamamura, Phys. Rev. B **95**, 155138 (2017).

[20] J. Pospíšil, Y. Haga, A. Miyake, S. Kambe, N. Tateiwa, Y. Tokunaga, F. Honda, A. Nakamura, Y. Homma, M. Tokunaga, D. Aoki, and E. Yamamoto, Phys. B: Condens. Matter **536**, 532 (2018).

[21] D. Hovančík, A. Koriki, A. Bendová, P. Doležal, P. Proschek, M. Míšek, M. Reiffers, J. Prokleška, J. Pospíšil, and V. Sechovský, Phys. Rev. B **105**, 014436 (2022).

[22] J. Pospíšil, Y. Haga, A. Miyake, S. Kambe, Y. Tokunaga, M. Tokunaga, E. Yamamoto, P. Proschek, J. Volný, and V. Sechovský, Phys. Rev. B **102**, 024442 (2020).

[23] K. Prokeš, A. de Visser, Y. K. Huang, B. Fåk, and E. Ressouche, Phys. Rev. B **81**, 180407(R) (2010).

[24] M. W. Butchers, J. A. Duffy, J. W. Taylor, S. R. Giblin, S. B. Dugdale, C. Stock, P. H. Tobash, E. D. Bauer, and C. Paulsen, Phys. Rev. B **92**, 121107(R) (2015).

[25] M. Taupin, J.-P. Sanchez, J.-P. Brison, D. Aoki, G. Lapertot, F. Wilhelm, and A. Rogalev, Phys. Rev. B **92**, 035124 (2015).

[26] It has been reported from the PND experiment that the direction of the magnetic moment at the Co site reorients antiparallel to that at the U site in the FM state, in agreement with first-principles calculations based on density-functional theory [27], although both sites are parallel in the paramagnetic state [23]. From the combination of the MCS and soft x-ray XMCD experiments, the magnetic moments at both sites are aligned in parallel in the FM state [24]. However, it is strange that the XMCD signals at U-N_5 are not observed, even below T_{Curie}, although the XMCD signals at Co-$L_{2,3}$ are detected clearly [24]. On the other hand, in the hard x-ray XMCD experiment [25], the XMCD signals at U-M_5 are detected distinctly, unlike the above-mentioned soft x-ray XMCD experiment.

[27] M. Diviš, Phys. B: Condens. Matter **403**, 2505 (2008).

[28] M. Vališka, J. Pospíšil, A. Stunault, Y. Takeda, B. Gillon, Y. Haga, K. Prokeš, M. M. Abd-Elmeguid, G. Nénert, T. Okane, H. Yamagami, L. Chapon, A. Gukasov, A. Cousson, E. Yamamoto, and V. Sechovský, J. Phys. Soc. Jpn. **84**, 084707 (2015).

[29] A. E. Dwight, P. P. Vaishnava, C. W. Kimball, and J. L. Matykiewicv, J. Less-Common Met. **119**, 319 (1986).

[30] K. Karube, T. Hattori, Y. Ihara, Y. Nakai, K. Ishida, N. Tamura, K. Deguchi, N. K. Sato, and H. Harima, J. Phys. Soc. Jpn. **80**, 064711 (2011).

[31] Y. Saitoh, Y. Fukuda, Y. Takeda, H. Yamagami, S. Takahashi, Y. Asano, T. Hara, K. Shirasawa, M. Takeuchi, T. Tanaka, and H. Kitamura, J. Synchrotron Radiat. **19**, 388 (2012).

[32] Y. Takeda, T. Okane, Y. Saitoh, H. Yamagami, E. Yamamoto, and Y. Haga, Prog. Nucl. Sci. Technol. **5**, 171 (2018).

[33] The magnitude of the XMCD intensity of UGe$_2$ Ge-$L_{2,3}$ is about four times larger than that of UCoGe and U(CoRu)Ge, which reflects the large magnitude of the magnetic moment of UGe$_2$ with $\sim 1.7 \mu_B$.

[34] K. Yamagami, Y. Fujisawa, B. Driesen, C. H. Hsu, K. Kawaguchi, H. Tanaka, T. Kondo, Y. Zhang, H. Wadati, K. Araki, T. Takeda, Y. Takeda, T. Muro, F. C. Chuang, Y. Niimi, K. Kuroda, M. Kobayashi, and Y. Okada, Phys. Rev. B **103**, L060403 (2021).

[35] T. Yoshikawa, V. N. Antonov, T. Kono, M. Kakoki, K. Sumida, K. Miyamoto, Y. Takeda, Y. Saitoh, K. Goto, Y. Sakuraba, K. Hono, A. Ernst, and A. Kimura, Phys. Rev. B **102**, 064428 (2020).

[36] P. Carra, B. T. Thole, M. Altarelli, and X. Wang, Phys. Rev. Lett. **70**, 694 (1993).

[37] B. T. Thole, P. Carra, F. Sette, and G. van der Laan, Phys. Rev. Lett. **68**, 1943 (1992).

[38] Y. Takeda, Y. Saitoh, T. Okane, H. Yamagami, T. D. Matsuda, E. Yamamoto, Y. Haga, Y. Ōnuki, and Z. Fisk, Phys. Rev. B **88**, 075108 (2013).

[39] Y. Takeda, Y. Saitoh, T. Okane, H. Yamagami, T. D. Matsuda, E. Yamamoto, Y. Haga, and Y. Ōnuki, Phys. Rev. B **97**, 184414 (2018).

[40] C. Felser and A. Hirobata, *Heusler Alloys: Properties, Growth, Applications* (Springer, New York, 2015), p. 15.

[41] C. T. Chen, Y. U. Idzerda, H.-J. Lin, N. V. Smith, G. Meigs, E. Chaban, G. H. Ho, E. Pellegrin, and F. Sette, Phys. Rev. Lett. **75**, 152 (1995).

[42] P. Gambardella, S. S. Dhesi, S. Gardonio, C. Grazioli, P. Ohresser, and C. Carbone, Phys. Rev. Lett. **88**, 047202 (2002).

[43] D. Hovančík, J. Pospíšil, K. Carva, V. Sechovský, and C. Piamonteze, Nano Lett. **23**, 1175 (2023).

[44] F. Wilhelm, J. P. Sanchez, J.-P. Brison, D. Aoki, A. B. Shick, and A. Rogalev, Phys. Rev. B **95**, 235147 (2017).

[45] S.-i. Fujimori, T. Ohkochi, I. Kawasaki, A. Yasui, Y. Takeda, T. Okane, Y. Saitoh, A. Fujimori, H. Yamagami, Y. Haga, E. Yamamoto, and Y. Ōnuki, Phys. Rev. B **91**, 174503 (2015).

[46] M. B. S. Neto, A. H. C. Neto, J. S. Kim, and G. R. Stewart, J. Phys.: Condens. Matter **25**, 025601 (2013).